Received: 19 October 2017 | Revised: 7 March 2018 | Accepted: 8 March 2018

DOI: 10.1002/rra.3282

RESEARCH ARTICLE

WILEY

The impact of climate change on the morphology of a tidal freshwater wetland affected by tides, discharge, and wind

E. Verschelling[1,2] | M. van der Perk[1] | H. Middelkoop[1]

[1] Department of Physical Geography, Utrecht University, Utrecht, the Netherlands

[2] Deltares, Delft, Netherlands

Correspondence
E. Verschelling, Department of Physical Geography, Utrecht University, Utrecht, the Netherlands.
Email: e.verschelling@uu.nl

Funding information
Dutch Technology Foundation STW, Grant/Award Number: 12431

Abstract

Tidal freshwater wetlands are threatened by climate change, especially by rising sea levels. Until now, research in these wetlands has focused mostly on determining historical and present-day accretion rates without analysing the influence of climate change on future developments. We study a recently constructed freshwater wetland under influence of tides, wind, and riverine discharges and carry out a scenario analysis to evaluate the impact of climate change on morphodynamics. We use a numerical model that describes the hydrodynamics and morphology in the study area and includes the impact of vegetation and carry out transient scenario runs for the period 2015–2050 with gradually changing boundary conditions. We conclude that the simulated accretion rates are significantly lower than the rate of sea level rise, meaning that the wetland will gradually convert to open water. We also find that the morphological changes can largely be attributed to morphological stabilization of the constructed wetland and not to climate change. Wind plays an important role through resuspension and redistribution of fine sediment, and neglecting it would lead to a significant overestimation of accretion rates on the flats.

KEYWORDS

climate change, De Biesbosch National Park, morphodynamics, numerical modelling, sea level rise, sediment deposition, tidal freshwater wetlands

1 | INTRODUCTION

Tidal wetlands are threatened by a combination of sea level rise, sediment starvation, and subsidence (e.g., Beckett, Baldwin, & Kearney, 2016; Belliard, Di Marco, Carniello, & Toffolon, 2016; Delgado, Hensel, Swarth, Ceroni, & Boumans, 2013; Kirwan & Megonigal, 2013). Survivability of coastal wetlands in the face of relative sea level rise (SLR and subsidence combined) has been studied extensively and depends on factors such as the availability of sediment (Neubauer, Anderson, Constantine, & Kuehl, 2002), wetland elevation (Temmerman, Govers, Wartel, & Meire, 2003), vegetation cover (Belliard et al., 2016; Gedan, Kirwan, Wolanski, Barbier, & Silliman, 2010), subsidence (Beckett et al., 2016), and the ability of the wetland to move in landward direction (Fagherazzi, Mariotti, Wiberg, & McGlathery, 2013; Kirwan & Megonigal, 2013). Tidal freshwater wetlands (TFWs) in the transition zone between *tidally dominated* and *fluvially dominated* sections of a river delta have received less attention in scientific literature.

Depending on wetland location and properties, flooding and sedimentation in TFWs are governed by the combined influence of tides, riverine discharges, and wind (Verschelling, Van der Deijl, Van der Perk, Sloff, & Middelkoop, 2017). Drowning mechanisms and measures that mitigate the impact of climate change (CC) in these areas, therefore, differ significantly from those in coastal areas, especially if CC also impacts river discharges and wind. Most research in TFWs has focused on understanding historical and present-day sedimentation rates and patterns and has shown that sedimentation rates depend on factors

such as supply of sediment (Neubauer et al., 2002), impact of tides and wind (Orson, Simpson, & Good, 1990; Vandenbruwaene et al., 2011; Verschelling et al., 2017), and wetland parameters such as average water depth, wind fetch lengths, and distance to creeks (Delgado et al., 2013; Hupp & Bazemore, 1993; Temmerman et al., 2003).

This paper focuses on the long-term effects of CC on the morphology of freshwater wetlands. More specifically, our objective is to understand and quantify the effects of CC on the morphology of a freshwater wetland affected by discharges, tides, and wind. To this end, we use a small microtidal flow-through wetland, located in the Biesbosch National Park in the Rhine–Meuse delta in the Netherlands, as a case study and compared net sediment deposition rates and sedimentation patterns of two distinct CC scenarios to present-day climate conditions. For this analysis, we deployed a numerical model that accounts for the interactions between hydrodynamics, morphology, and vegetation. We carried out transient scenario runs for the period 2015–2050, in which the boundary conditions changed on a yearly basis, using synthetic yearly time series of discharge, water level, and wind with similar statistical properties (auto and cross correlations) as the original measured time series. The simulation results were then post-processed to net sedimentation/erosion patterns over the years and bed levels and the evolution of average and flat levels over time. Finally, we tested the sensitivity of the accretion rates to an alternative vegetation scenario and to the impact of wind.

2 | STUDY AREA

The study area consists of a number of former polders in the Biesbosch National Park, a 9,000 ha tidal freshwater wetland in the lower Rhine and Meuse delta in the Netherlands (Figure 1). During 2007–2008, a channel network was constructed through the polders, and the embankments were opened at the northern and southern sides of the area, connecting the newly created wetland to the river Nieuwe Merwede and Gat van de Noorderklip, respectively. The objective of this opening was to lower upstream flood levels by enlarging local conveyance capacity of the river Rhine. Due to the location of the newly created wetland in the backwater of the North Sea (Kleinhans, Weerts, & Cohen, 2010), it is potentially threatened by SLR, making it a relevant study area. It has a limited number of connections to the surrounding water system, which facilitates the construction of sediment and water balances.

The flow-through wetland has a surface area of about 700 ha and has a dominant flow direction from north to south. The sandy material that was dug from the channels was used to create an artificial island in the centre of the area. The rest of the area has an average surface level of 0.3 m above the Dutch Ordnance Datum (NAP) and consists of mud flats still covered by the original layer of polder clay. The channels occupy around 25% of the surface area of the study area. Tides in the region are semidiurnal with a typical range between 0.2 and 0.4 m. Average depth on the tidal flats ranges from 0 to 0.5 m. Occasional exposure of the flats occurs at low tide or during easterly winds in the summer. Water levels in the area are strongly affected by Rhine discharge and tides. Storm surges from westerly winds at sea occasionally cause large setup in the wetland. Winds play an important role in shaping the morphodynamics of the system. Locally generated wind waves cause a substantial amount of resuspension due to the long fetch lengths across the inundated flats (Verschelling et al., 2017).

Suspended sediment concentrations (SSCs) at the inlet of the system typically vary from 10 to 40 mg/L during average flow conditions. During peak discharges, SSCs in the upstream Rhine River can reach up to 140 mg/L (Asselman, 2000). Since the de-embankment of the area in 2008, sedimentation has taken place in the central section of the channel system with values up to 14.3 mm/year, whereas channel sections close to the inlet and outlet have experienced significant erosion (van der Deijl, van der Perk, & Middelkoop, 2017). The flats have remained relatively intact due to the erosion resistance of the layer of polder clay in combination with low flow velocities. Since 2008, most of the flats have been covered by a layer of mud 2 to 5 cm thick, with most of the aggradation occurring close to the channels (Verschelling et al., 2017). We refer to van der Deijl et al. (2017) and Verschelling et al. (2017) for more details on the morphological evolution in the study site.

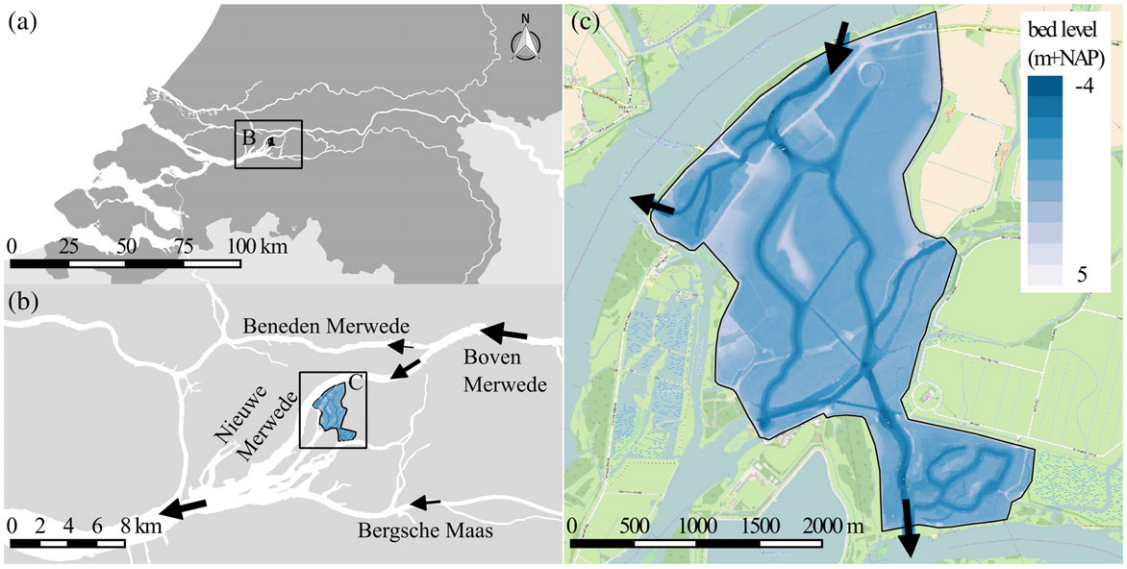

FIGURE 1 Study area. The arrows indicate the main flow directions [Colour figure can be viewed at wileyonlinelibrary.com]

Vegetation in the study area is sparse. It consists mostly of shrublands and softwood riparian forests on the higher grounds, reed fields, pioneer herbs, and multiple types of grassland on the banks along the island and the flats and multiple species of mudwort and macrofytes on the flats (Van der Werf, 2016). Currently, vegetation is kept short by grazing (cows and geese) and by mowing. This effectively removes most of the vegetation from the mudflats and the island and also conserves the grassland.

3 | METHODS

3.1 | Model setup and calibration

We used the depth-averaged version of the Delft3D modelling framework (Lesser, Roelvink, van Kester, & Stelling, 2004) to simulate water flow, sediment transport, and bed level changes in the study area. Here, we provide a short overview of the model setup and calibration, both of which are described in more detail by Verschelling et al. (2017).

Bed level changes are simulated based on differences in sediment transport rates of cohesive and noncohesive sediment fractions, calculated with the Krone and Ariathurai–Partheniades equations (Partheniades, 1965) and the Van Rijn (1984) equation, respectively. The SWAN wave model (available in Delft3D as Delft3D WAVE) was used to account for the impact of wind-generated waves on hydromorphodynamics. The computational grid covers the study area as highlighted in Figure 1c. It is a curvilinear grid with 144 × 145 cells and has cell sizes ranging from 5 to 30 m. The initial bathymetry was constructed by combining a 2011 dataset describing the channel bathymetry, the 2003 version of the official Dutch digital elevation model ("AHN1"), and a local 2010 LiDAR digital elevation model of the higher grounds in the system (Verschelling et al., 2017). These datasets were provided by the Dutch National Water Authority (*Rijkswaterstaat*). Initial bed composition consisted of one uniformly mixed layer of two sediment fractions (one cohesive mud fraction and one noncohesive sand fraction) with 100% mud on the flats and 100% sand in the rest of the system (channels and island). The hydrodynamic and sediment transport models were calibrated and validated for periods in 2011, 2014, and 2015. The hydrodynamic model calibration was carried out for measured water level series at three gauging stations and resulted in root-mean-square error values ranging from 0.46 to 1.80 cm. The calibration of the sediment transport model yielded a Brier skill score of 0.81, which means that the model performance can be classified as "good" (Verschelling et al., 2017).

3.2 | Scenario calculations

We used the so-called *2050GL* and *2050WH* CC scenarios developed for the Netherlands by the Royal Netherlands Meteorological Institute (KNMI; Van den Hurk, Siegmund, Klein Tank, & Attema, 2014). The 2050GL scenario expects low changes in air circulation patterns combined with moderate rise of global temperature, which translates into a 4% increase in precipitation and 0.15 to 0.3 m increase in mean sea level at the North Sea coast compared with the reference climatic period, 1981–2010 (Van den Hurk et al., 2014). The 2050WH scenario combines a relatively large rise of global temperature with changes in atmospheric circulation patterns, leading to 5% more precipitation and an increase in mean sea level of 0.2 to 0.4 m. For the purpose of this scenario analysis, we chose to use the most extreme values of expected SLR (0.3 m for 2050GL and 0.4 m for 2050WH). For reference, we also included a 2050 scenario without any CC (*2050REF*). We chose 2015–2050 as scenario period, because 2050 is a horizon year that fits well with the KNMI scenarios and is commonly used in climate scenario research projects (e.g., Parry, Canziani, Palutikof, van der Linden, & Hanson, 2007).

Model boundary conditions for the 2015–2050 simulations consisted of yearly synthetic time series of discharges at the upstream boundary (river Nieuwe Merwede), water levels at the downstream boundary (creek Gat van de Noorderklip), and west-northwest winds over the entire model domain (Table 1). These time series were constructed through linear interpolation between 2015 and the two-scenario-2050 time series.

The 2015, 2050GL, and 2050WH time series were constructed as follows. First, we used scenario-specific time series for the period 1-1-1967 to 1-1-2007 of the daily discharge at Lobith (Location a in Figure 2) developed by Sperna Weiland, Hegnauer, Bouaziz, and Beersma (2015), 2-hourly tidal water levels at Hoek van Holland (Location b) and Haringvliet-buiten (Location c) provided by the Dutch department of waterways and public works (Rijkswaterstaat,

TABLE 1 Overview of scenarios and their boundary conditions

	2015 boundaries		2050 boundaries		
Scenario	Q & h	Wind	Q & h	Wind	Vegetation
2050REF	2015	2015	2015	2015	2015
2050GL	2015	2015	2050gl	2015	2015
2050WH	2015	2015	2050wh	2015	2015
2050NOWIND	2015	-	2015	-	2015
2050GRAZING	2015	2015	2015	2015	No grazing

Note. h = water level; Q = water discharge. Scenarios 2050NOWIND and 2050GRAZING are described in Section 5 and included here for completeness.

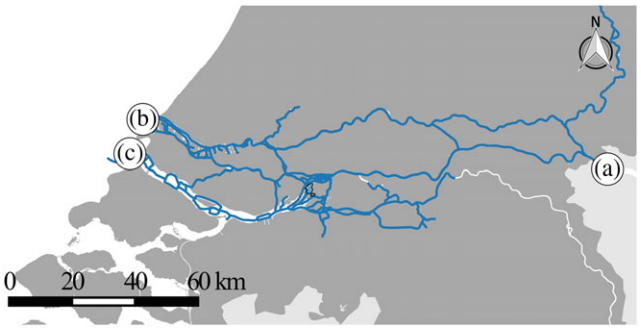

FIGURE 2 Extent of the 1D model (in blue) and locations of 1D model boundary conditions: Lobith (a), Hoek van Holland (b), and Haringvliet-buiten (c) [Colour figure can be viewed at wileyonlinelibrary.com]

TABLE 2 Statistical properties of the original time series for the present-day (2015) climate and the synthetic version of these series

Parameter		Avg	SD	Sk (–)	T_{ac} (d)	$C_{mx}Q$ (–)	$C_{mx}H$ (–)	$C_{mx}U$ (–)
		Original time series 2015						
Discharge upstream	m^3/s	71.5	60.5	0.9	20.0	-	0.45	0.18
Water level downstream	m + NAP	0.49	0.27	0.79	4.0	0.45	-	0.55
WNW wind velocity	m/s	0.88	3.51	0.46	1.0	0.18	0.55	-
		Synthetic time series 2015						
Discharge upstream	m^3/s	71.5	48.5	2.2	20.0	-	0.67	0.41
Water level downstream	m + NAP	0.49	0.23	1.07	4.0	0.67	-	0.73
WNW wind velocity	m/s	0.92	3.51	0.46	1.0	0.41	0.73	-

Note. AvG = average, SD = standard deviation, Sk = skewness, T_{ac} = autocorrelation time. $C_{mx}Q$, $C_{mx}H$, and $C_{mx}U$ are the maximum correlations with discharge upstream, water level downstream, and WNW wind velocity, respectively. A similar comparison for the other two sets of time series (2050wh and 2050gl) gave similar differences and is therefore omitted from this table.

2016), and the 2-hourly wind speed and velocity at four surrounding stations provided by KNMI (KNMI, 2016). Second, we routed those signals to the boundary locations of our Delft3D model using a 1D model of the Dutch river network, described in (Chbab, 2012).

Third, we constructed synthetic time series of 2-hourly discharges, water level, and wind speed (assuming dominant wind direction of WNW) with a duration of 1 year using an approach described in detail in Van den Boogaard, Uittenbogaard, and Mynett (2003). This approach consists of an iterative optimization algorithm that uses random seeds to construct synthetic time series that satisfy several a priori defined statistical properties. In this case, those properties are the marginal probability density distribution and auto-covariance function of the routed signals at the locations of the Delft3D boundaries. For the water level, a distinction was made between a so-called carrier signal (setup) and a residual signal (tide). Although the algorithm was originally developed for univariate distributions only, we manually checked for cross correlations between the discharge, water level, and wind speed. This is important because in our case, these variables are correlated due to the location of our

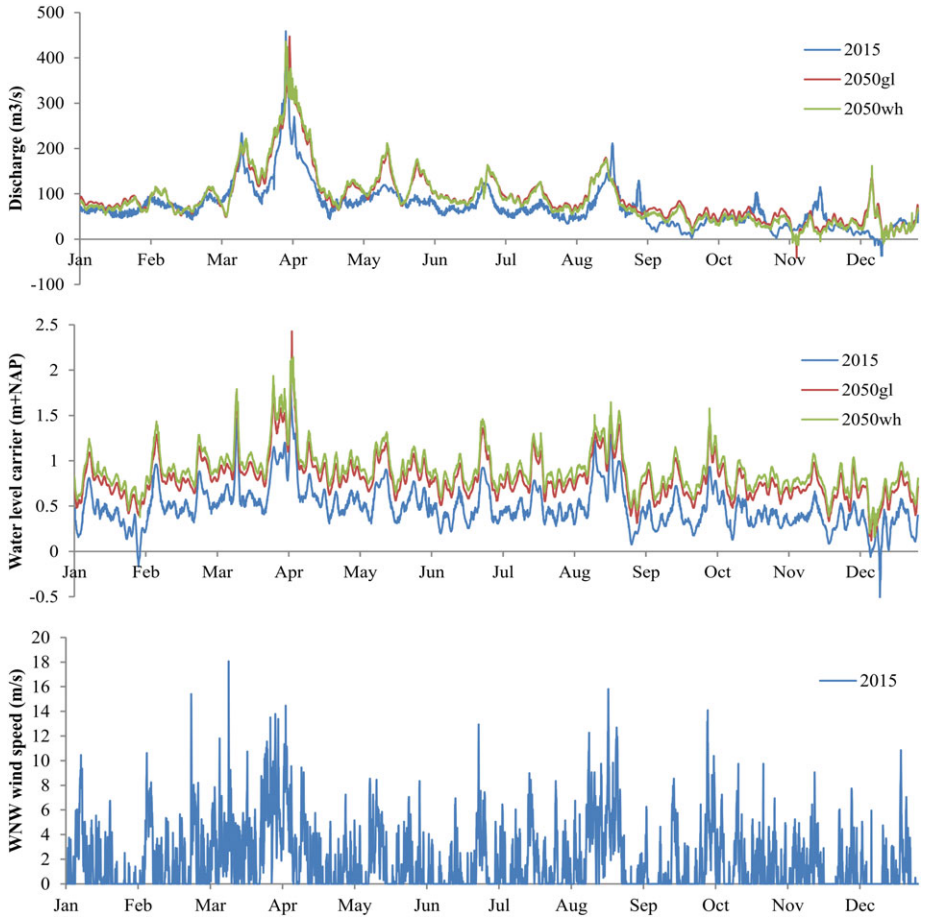

FIGURE 3 Yearly synthetic time series of discharge, water level (carrier), and wind velocity for 2015, 2050gl, and 2050wh [Colour figure can be viewed at wileyonlinelibrary.com]

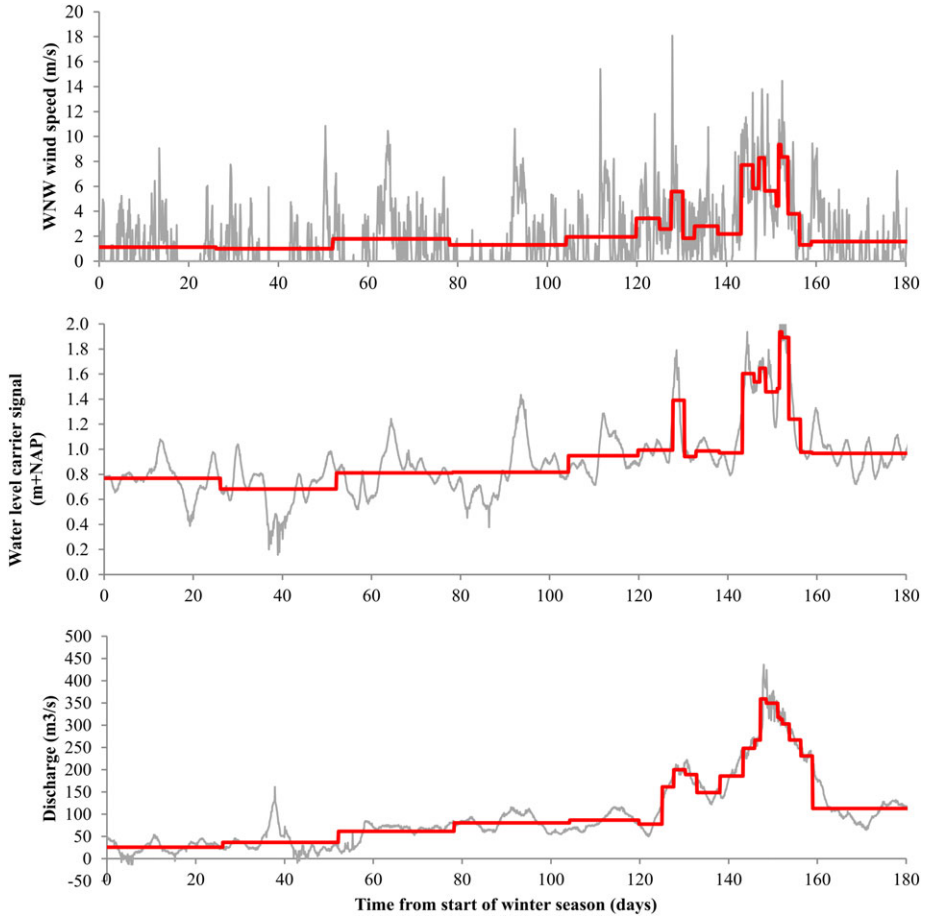

FIGURE 4 Synthetic time series (in grey) and stepwise compressed series (in red) of wind speed, water level (carrier), and discharge for the 2050WH/winter scenario. Every step of the compressed series represents 12 hr 25 min (one tidal cycle) simulation time with a corresponding value of the morphological factor: the longer the step, the larger the morphological factor. Note that the compressed series consists of 21 steps, which means that the simulation time of a winter season is almost 11 days with an average morphological factor of 17 [Colour figure can be viewed at wileyonlinelibrary.com]

study area at the transition point between the discharge-dominated and tidally dominated parts of the river system. We therefore constructed six alternative sets of time series and then selected the sets of time series that best satisfied the cross-correlations of the original dataset. A comparison between statistical properties of the original time series and the synthetic versions is given in Table 2, and Figure 3 shows the synthetic time series.

Fourth, we split each of these time series into a summer season (May–October) and a winter season (November–April). Although we could have used these time series to carry out the scenario analysis, this would have been very impractical due to the long calculation times. As a fifth step, we therefore applied a compression technique to the time series using a variable morphological multiplication factor in the range from 1 to 50 with a yearly average value of 21, leading to stepwise compressed time series of discharge, water level carrier, and wind speed (Figure 4). Finally, a harmonic tidal signal was superimposed on the water level carrier time series, similar to the approach described by Verschelling et al. (2017). This resulted in compressed time series for both seasons for all scenarios. Boundary conditions for individual simulations in 2015–2050 were derived from these time series by linear interpolation.

The suspended sediment concentrations at the upper model boundary locations were defined using the sediment rating curves constructed previously by Verschelling et al. (2017).

3.3 | Vegetation

We modelled the hydraulic resistance due to vegetation using the Baptist equation (Baptist et al., 2007), which distinguishes between flow-through and flow-over vegetation and links hydraulic resistance to vegetation parameters such as height, stem diameter, and density. The impact of vegetation on reduction of wave energy was modelled in the Delft3D WAVE module using the model developed by Suzuki, Zijlema, Burger, Meijer, and Narayan (2012), which requires the same vegetation parameters as the Baptist equation.

Initial simulations showed that changes in abiotic conditions during the scenario period (2015–2050) will likely not lead to significant vegetation succession in the area or an increase in vegetation cover in the currently sparsely vegetated area. On the contrary, some loss of vegetation is expected due to elevated water levels. We therefore decided not to include a separate vegetation growth module in the model simulations to periodically update vegetation patterns based on changes in abiotic conditions and vegetation succession

TABLE 3 (a) Key vegetation species habit suitability rules and (b) key vegetation properties

Vegetation type	Key species	Minimum required bed level	Maximum required bed level
Riparian forest	*Salix alba*	>0 m MHW	<1.4 m MHW
Helophytes	*Phragmites australis*	>0 m MW	<0.2 m MW
Shrubland	*Urtica dioica*	>0.5 m MHW	-
Submerged vegetation	*Macrophytes Potamogeton*	>−1.5 m MW	<−0.2 m MW
Pioneer herbaceus plants	*Pioneer herbs*	>0 m MHW	-
Grassland	*Lolium perenne*	>0.2 m MHW	-

	General		Summer			Winter		
Key species	Diameter (m)	Cb ($m^{0.5}/s$)	# stems (/m2)	height (m)	drag (−)	# stems (/m2)	height (m)	drag (−)
Salix alba	0.18	18	0.16	20	2	0.16	20	1.5
Phragmites australis	0.004	30	100	2.5	2	100	2.5	1
Urtica dioica	0.008	30	100	1.5	2	32	1	1
Macrophytes Potamogeton	0.005	40	75	1	2	-	-	-
Pioneer herbs	0.003	30	50	1	2	50	0.15	1
Lolium perenne	-	30	-	-	-	-	-	-

knowledge rules. Instead, we used a fixed vegetation pattern for the entire period, based on the expected abiotic conditions halfway through the scenario period (2033). We constructed this vegetation cover as follows: first, we selected six representative vegetation types, and for each of these types, a key species was selected to represent that type (Table 3a). For each of the key vegetation species, the relevant parameters for the hydraulic roughness and wave damping formulations in Delft3D were defined based on Van Velzen, Jesse, Cornelissen, and Coops (2003), Oorschot, Kleinhans, Geerling, and Middelkoop (2015), and Van der Werf (2016; Table 3b). A distinction was made between summer and winter parameter values to account for the varying properties of certain vegetation types between the two seasons (leaves or no leaves and plants or no plants in the case of macrophytes). Next, we constructed a vegetation cover for these species according to the most recent local vegetation surveys (Bijkerk & Davids, 2012; Everts & De Vries, 2011) and assumed this to be representative for the 2015 vegetation cover (Figure 5a). This 2015 vegetation cover is partly determined by the grazing of cows and geese, leading to the continued existence of patches of grass on the higher grounds and to a reduction of macrophytes and pioneer vegetation on the inundated flats. Because initial simulations showed that water depths in the wetland are likely to increase, we decided to use a realistic vegetation scenario for the 2015–2050 period, which would maximize sedimentation. This scenario assumes cows to be prevented from grazing, whereas the increased water depths would prevent the geese from removing all of the macrophytes on the flats, which lead to succession of grass by shrubs and growth of macrophytes on the inundated flats. We implemented this vegetation scenario by modifying the 2015 vegetation cover according to a set of numerical knowledge rules based on

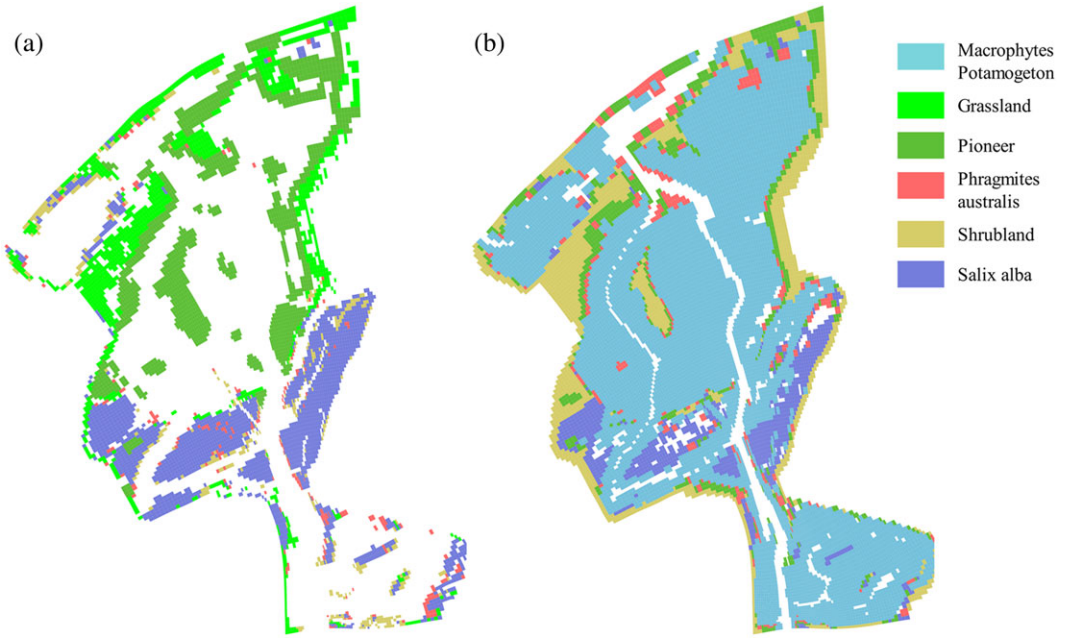

FIGURE 5 (a) Vegetation cover as surveyed in 2010/2011 and (b) as used in the summer calculations of scenarios 2050REF, 2050WH, and 2050GL. The vegetation cover for the winter calculations is identical to that of the summer except for the absence of Macrophytes Potamogeton. The 2010/2011 survey did not include Macrophytes species [Colour figure can be viewed at wileyonlinelibrary.com]

the work of Van der Werf (2016) that expresses habitat suitability in terms of abiotic conditions (Table 3a) to arrive at the fixed cover for the 2015–2050 scenarios (Figure 5b).

4 | RESULTS

For all scenarios, most of the changes in morphology occur in the channel system between −0.5 m NAP (Figure 6a) and 0.3 m NAP and below −3 m NAP (not shown in Figure 6): they become narrower and deeper. Compared with the 2050REF, the 2050WH and 2050GL scenarios both lead to enhanced sedimentation on the channel banks and an elevated bed level of the flats. Nevertheless, the difference between 2015 and 2050REF is much larger than the difference between 2050REF and 2050WH or 2050GL, implying that most of the morphological changes in the area can be attributed to morphological stabilization of the relatively recently reclaimed wetland and not as much to the impact of CC.

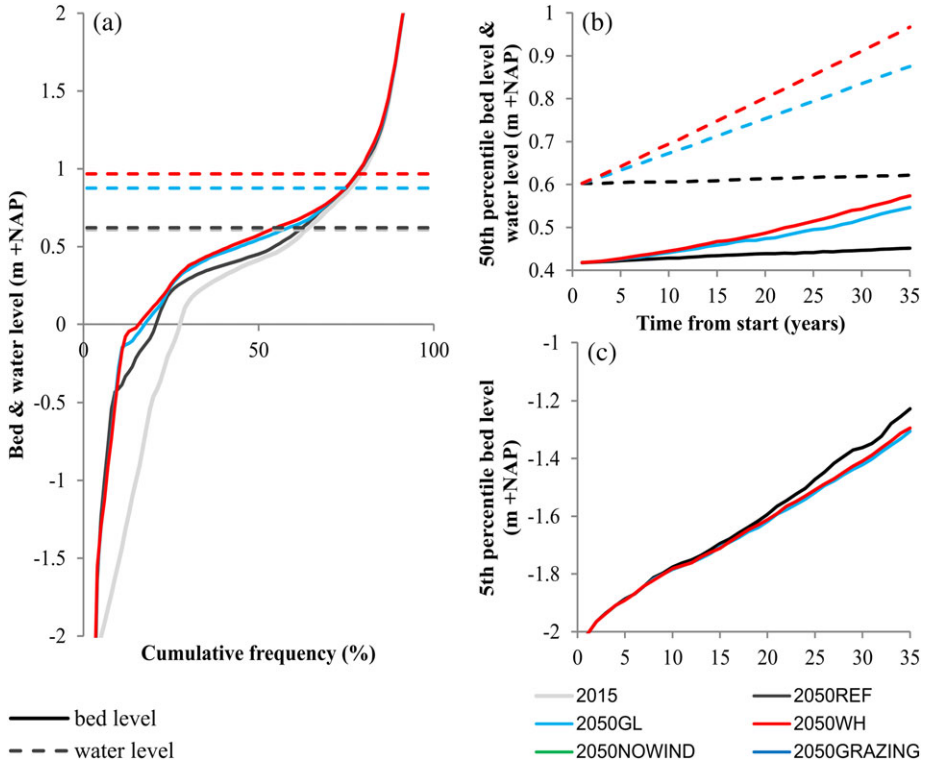

FIGURE 6 (a) 2015 and 2050 bed level cumulative frequency distributions and water levels for climate change scenarios, (b) and (c) 5th and 50th percentile bed levels and water levels for climate change scenarios [Colour figure can be viewed at wileyonlinelibrary.com]

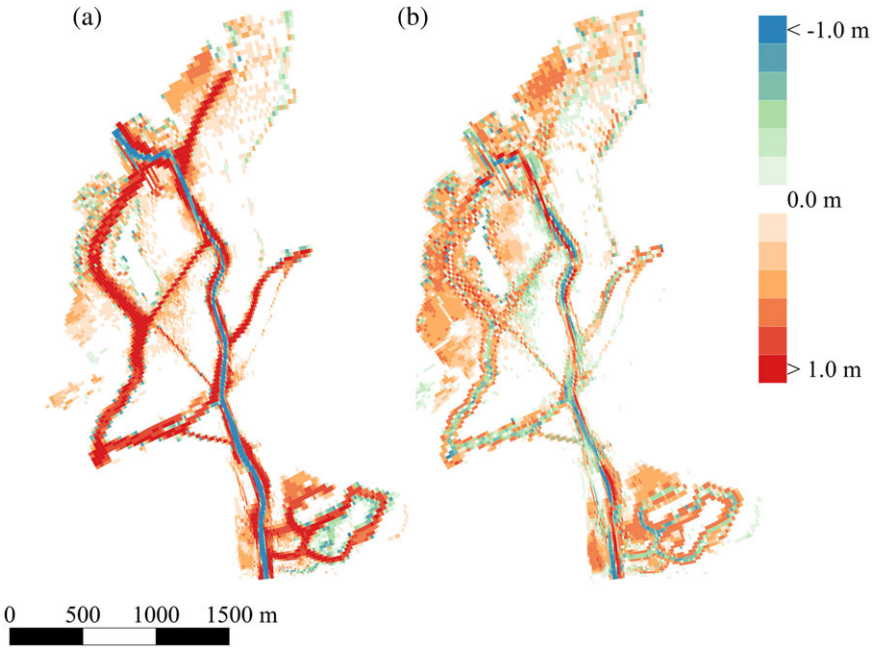

FIGURE 7 Sedimentation/erosion patterns of the scenario runs over the period 2015–2050. (a) shows bed level changes for reference scenario 2050REF (2050REF minus 2015), (b) shows impact of 2050WH compared with 2050REF (2050WH minus 2050REF) [Colour figure can be viewed at wileyonlinelibrary.com]

Figure 6b,c shows the development of the average water levels and the 5th and 50th percentile bed levels for the three scenario runs. We assume these percentiles to be representative of channel bed and flat bed levels, respectively. For both CC scenarios, the level of the flats is unable to keep pace with the rise in water levels (GL: 0.05 vs. 0.27 m and WH: 0.06 vs. 0.36 m). For all scenario runs, the evolution of both the channel bed and the flat bed is almost linear, indicating that the morphological system is still far from stable.

In the 2050REF scenario, most of the changes take place in and around the channel system (Figure 7a). Most of the channels have become narrower and slightly deeper, except for the western branch, which has filled up with sediment due to lower flow velocities compared with eastern channel. The 2050WH CC scenario leads to more erosion in the eastern channel and more sedimentation in the western channel compared with 2050REF. The pattern of scenario 2050GL is very similar and is therefore not shown. The differences on the flats are limited to a slight increase in sedimentation on the flats in the NW and the SE, which are most protected from the wind.

5 | DISCUSSION

The current mean accretion rate on the intertidal flats in our study area is about 6 mm/year, which is just sufficient to keep up with the current rate of SLR (van der Deijl et al., 2017). However, our results show that this rate will quickly drop to about 1 mm y^{-1} for the period 2015–2050 for the two CC scenarios. These rates are substantially lower than the local rate of SLR (2050GL: 8 mm/year and 2050WH: 10 mm/year), which implies that this marsh will likely gradually convert to open water over decades.

Because the bed level changes of the 2050REF scenario are much larger than the difference between 2050REF and 2050WH or 2050GL scenarios, most of the morphological changes in the relatively recently constructed Kleine Noordwaard wetland over the period 2015–2050 can be attributed to morphological stabilization and not to the impact of CC. CC does however increase the rate of these changes, especially in the western branch of the channel system: these tend to fill up more rapidly under CC. We speculate that this process will likely continue beyond 2050, up to a point where it starts to limit the water discharge into the system and with it, the influx of sediment.

The current sedimentation rates in the study area fall within the range of rates reported for other sites along the lower Rhine branches, such as a de-embanked polder with the rate of 1–2 mm/year (Bleuten, Borren, Kleinveld, Oomes, & Timmermann, 2009) and the floodplains along the river Waal with rates between 0.2 and 11.6 mm/year (Middelkoop, 1997). These values are low compared with accretion rates found for freshwater marshes in the USA which vary between 1 and 27 mm/year (Delgado et al., 2013; Mitsch et al., 2014; Orson et al., 1990). Sediment starvation often plays a large role in reduced sedimentation rates (Neubauer et al., 2002). This is also the case for the river Rhine, where upstream river regulation works have led to a significant drop in SSCs over the last decades (Snippen et al., 2005; Vollmer & Goelz, 2006). Current SSC at the inlet of our study area averages at about 15 mg/L, which is very low compared with other TFWs (van der Deijl et al., 2017).

Our study is one of the first where the impact of CC on the sediment budget of a microtidal freshwater wetland is quantified. Coastal wetlands have been studied more extensively and often gain elevation at speeds similar to SLR due to ecogeomorphic feedback loops that cause increased deposition of both mineral sediment and organic material as the water depth increases (French, 2006; Kirwan & Megonigal, 2013). However, these feedback loops only occur until a certain flooding threshold, beyond which the vegetation dies off and the feedbacks are stopped, causing wetlands to drown (Kirwan & Megonigal, 2013). For coastal wetlands, this threshold can be reached in case of very high rates of local SLR, in some cases causing wetland submergence (Cahoon, Reed, & Day, 1995; Kirwan et al., 2010). For our constructed microtidal TFW, we speculate that design decisions made prior to the de-embankment have led to an immediate overtopping of the flooding threshold, prohibiting such feedback that may have promoted accretion, but instead have led to large scale vegetation die-off.

Wind has been identified as an important driver for erosion in coastal marshes and mud flats (e.g., Mariotti & Fagherazzi, 2010; Tonelli, Fagherazzi, & Petti, 2010) but has received little attention in scientific studies on tidal freshwater wetlands. Verschelling et al. (2017) carried out a sensitivity analysis on the short-term impact of wind events in the study area and concluded that wind-driven short waves indeed lead to resuspension and subsequent outflow of significant amounts of fine sediment from the area. It is therefore likely that wind also reduces the long-term accretion rates under CC. We tested this hypothesis by running extra simulation 2050NOWIND, in which we switched off the wind forcing completely. This led to a relatively large increase in the 2015–2050 accretion rate (12.1 cm instead of 3.4 cm), which demonstrates the importance of including the impact of wind in the assessment of accretion rates in TFWs.

Our research suggests that it is important to ensure that abiotic conditions after de-embankment promote vegetation growth and succession in order to prevent drowning. This study also underlines the need to distinguish between the different components contributing to morphological changes: sedimentation patterns and rates are governed by a balance between boundary conditions (affected by external factors such as CC and anthropogenic modifications such as dams and gates) and internal conditions (such as the channel system and bed levels). Exciting future research directions would be to further assess the role of internal drivers such as wetland shape, channel configuration, and inlet sizes on the long-term accretion rates and patterns in TFWs.

6 | CONCLUSIONS

We carried out a scenario analysis to gain insight in the impact of CC on the morphology of a recently constructed TFW affected by a combination of tides, winds, and riverine discharges. The main conclusions are as follows:

- The scenario study shows that the simulated accretion rates over the scenario period are significantly lower than the rate of SLR for

the two CC scenarios. This means that the study area will gradually convert to open water.

- Nevertheless, CC leads to enhanced sedimentation on the channel banks and an elevated bed level of the flats.
- Most of the morphological changes that take place over the scenario period (2015–2050) can be attributed to morphological stabilization and not to CC.
  - Present-day abiotic conditions do not lead to vegetation succession and ecogeomorphic feedbacks that may promote increased accretion rates. Instead, the considerable water depth and inundation frequency lead to vegetation die-off and corresponding increase in wind shear.
- Neglecting the impact of wind leads to a significant overestimation of accretion rates.

ACKNOWLEDGEMENTS

This study was financed by the Dutch Technology Foundation STW (Project 12431). We thank Staatsbosbeheer and Rijkwaterstaat-WNZ for the provided data. We thank Bert Jagers, Henk van den Boogaard, Sofia Caires, and Karen Meijer (all from Deltares) for their help with Delft3D and the useful discussions. We thank Karianne van der Werf for her useful research on vegetation growth and succession in the study area.

ORCID

E. Verschelling http://orcid.org/0000-0002-2561-1831
M. van der Perk http://orcid.org/0000-0002-7968-661X
H. Middelkoop http://orcid.org/0000-0002-9549-292X

REFERENCES

Asselman, N. E. M. (2000). Fitting and interpretation of sediment rating curves. *Journal of Hydrology*, *234*, 228–248. https://doi.org/10.1016/S0022-1694(00)00253-5

Baptist, M. J., Babovic, V., Rodríguez Uthurburu, J., Keijzer, M., Uittenbogaard, R. E., Mynett, A., & Verwey, A. (2007). On inducing equations for vegetation resistance. *Journal of Hydraulic Research*, *45*, 435–450. https://doi.org/10.1080/00221686.2007.9521778

Beckett, L. H., Baldwin, A. H., & Kearney, M. S. (2016). Tidal marshes across a Chesapeake Bay Subestuary are not keeping up with sea-level rise. *PLoS One*, *11*, e0159753. https://doi.org/10.1371/journal.pone.0159753

Belliard, J. P., Di Marco, N., Carniello, L., & Toffolon, M. (2016). Sediment and vegetation spatial dynamics facing sea-level rise in microtidal salt marshes: Insights from an ecogeomorphic model. *Advances in Water Resources*, *93*, **Part B**, 249–264. https://doi.org/10.1016/j.advwatres.2015.11.020

Bijkerk, W., Davids, L. (2012). Vegetatiestructuurkartering Biesbosch, Pilotstudie naar de mogelijkheden van halfautomatische classificatie.

Bleuten, W., Borren, W., Kleinveld, E., Oomes, L. B., & Timmermann, T. (2009). Water and nutrient balances of the experimental site Mariapolder, The Netherlands. In A. Barendrecht, D. F. Whigham, & A. H. Baldwin (Eds.), *Tidal FreshwWetl* (pp. 167–206). Leiden: Backhuys Publishers. chap 18

Cahoon, D. R., Reed, D. J., & Day, J. W. (1995). Estimating shallow subsidence in microtidal salt marshes of the southeastern United States: Kaye and Barghoorn revisited. *Marine Geology*, *128*, 1–9. https://doi.org/10.1016/0025-3227(95)00087-F

Chbab, H. (2012). Achtergrondrapportage hydraulische belasting voor de Benedenrivieren. Deltares rapport 1204143–003:

Delgado, P., Hensel, P. F., Swarth, C. W., Ceroni, M., & Boumans, R. (2013). Sustainability of a tidal freshwater marsh exposed to a long-term hydrologic barrier and sea level rise. *Estuaries and Coasts*, *36*, 585–594. https://doi.org/10.1007/s12237-013-9587-2

Everts, F. H., De Vries, N. P. J. (2011). Vegetatiekartering Biesbosch & plantensoortkartering Kleine Noordwaard 2010.

Fagherazzi, S., Mariotti, G., Wiberg, P. L., & McGlathery, K. J. (2013). Marsh collapse does not require sea level rise. *Oceanography*, *26*, 70–77.

French, J. (2006). Tidal marsh sedimentation and resilience to environmental change: Exploratory modelling of tidal, sea-level and sediment supply forcing in predominantly allochthonous systems. *Marine Geology*, *235*, 119–136. https://doi.org/10.1016/j.margeo.2006.10.009

Gedan, K. B., Kirwan, M. L., Wolanski, E., Barbier, E. B., & Silliman, B. R. (2010). The present and future role of coastal wetland vegetation in protecting shorelines: Answering recent challenges to the paradigm. *Climatic Change*, *106*, 7–29. https://doi.org/10.1007/s10584-010-0003-7

Hupp, C. R., & Bazemore, D. E. (1993). Introduction to the 28th International Geological Congress Symposium on the Hydrogeology of Wetlands Temporal and spatial patterns of wetland sedimentation, West Tennessee. *Journal of Hydrology*, *141*, 179–196. https://doi.org/10.1016/0022-1694(93)90049-F

Kirwan, M. L., Guntenspergen, G. R., D'Alpaos, A., Morris, J. T., Mudd, S. M., & Temmerman, S. (2010). Limits on the adaptability of coastal marshes to rising sea level. *Geophysical Research Letters*, *37*. n/a-n/a. https://doi.org/10.1029/2010GL045489

Kirwan, M. L., & Megonigal, J. P. (2013). Tidal wetland stability in the face of human impacts and sea-level rise. *Nature*, *504*, 53–60. https://doi.org/10.1038/nature12856

Kleinhans, M. G., Weerts, H. J. T., & Cohen, K. M. (2010). Avulsion in action: Reconstruction and modelling sedimentation pace and upstream flood water levels following a Medieval tidal-river diversion catastrophe (Biesbosch, The Netherlands, 1421–1750AD). *Geomorphology*, *118*, 65–79. https://doi.org/10.1016/j.geomorph.2009.12.009

Royal Netherlands Meteorological Institute (2016). Uurgegevens van het weer in Nederland. http://www.knmi.nl/nederland-nu/klimatologie/uurgegevens. Downloaded at 8 july 2016.

Lesser, G. R., Roelvink, J. A., van Kester, J. A. T. M., & Stelling, G. S. (2004). Development and validation of a three-dimensional morphological model. *Coastal Engineering*, *51*, 883–915. https://doi.org/10.1016/j.coastaleng.2004.07.014

Mariotti, G., & Fagherazzi, S. (2010). A numerical model for the coupled long-term evolution of salt marshes and tidal flats. *Journal of Geophysical Research - Earth Surface*, *115*. n/a-n/a. https://doi.org/10.1029/2009JF001326

Middelkoop H (1997). Embanked floodplains in the Netherlands. Geomorphological evolution over various time scales. Phd thesis, Utrecht University, The Netherlands. Geographical Studies 224.

Mitsch, W. J., Nedrich, S. M., Harter, S. K., Anderson, C., Nahlik, A. M., & Bernal, B. (2014). Sedimentation in created freshwater riverine wetlands: 15 years of succession and contrast of methods. *Ecological Engineering*, *72*, 25–34. https://doi.org/10.1016/j.ecoleng.2014.09.116

Neubauer, S. C., Anderson, I. C., Constantine, J. A., & Kuehl, S. A. (2002). Sediment deposition and accretion in a mid-Atlantic (U.S.A.) tidal freshwater marsh. *Estuarine, Coastal and Shelf Science*, *54*, 713–727. https://doi.org/10.1006/ecss.2001.0854

Oorschot, M. V., Kleinhans, M., Geerling, G., & Middelkoop, H. (2015). Distinct patterns of interaction between vegetation and morphodynamics. *Earth Surface Processes and Landforms*, *41*, 791–808. https://doi.org/10.1002/esp.3864

Orson, R. A., Simpson, R. L., & Good, R. E. (1990). Rates of sediment accumulation in a tidal freshwater marsh. *Journal of Sedimentary Research*, *60*, 859–869.

Parry, M. L., Canziani, O. F., Palutikof, J. P., van der Linden, & Hanson, C. E. (Eds.). (2007). Climate Change 2007: Impacts, Adaptation and Vulnerability. Contribution of Working Group II to the Fourth Assessment Report of the Intergovernmental Panel on Climate Change, Cambridge University Press, Cambridge, UK, 982pp.

Partheniades, E. (1965). Erosion and deposition of cohesive soils. *Journal of the Hydraulics Division*, *91*, 105–139.

Rijkswaterstaat. (2016). Waterbase. http://live.waterbase.nl/. Downloaded at 14 september 2016.

Snippen, E., Fioole, A., Geelen, H., Kamsteeg, A., Van Spijk, A., Visser, T. (2005). Sediment in (be)weging. Sedimentbalans Rijn-Maasmonding periode 1990–2000 RWS-RIZA.

Sperna Weiland, F,. Hegnauer, M., Bouaziz, L., Beersma, J. (2015). Implications of the KNMI'14 climate scenarios for the discharge of the Rhine and Meuse. Deltares report 1220042–000.

Suzuki, T., Zijlema, M., Burger, B., Meijer, M. C., & Narayan, S. (2012). Wave dissipation by vegetation with layer schematization in SWAN. *Coastal Engineering*, *59*, 64–71. https://doi.org/10.1016/j.coastaleng.2011.07.006

Temmerman, S., Govers, G., Wartel, S., & Meire, P. (2003). Spatial and temporal factors controlling short-term sedimentation in a salt and freshwater tidal marsh, Scheldt estuary, Belgium, SW Netherlands. *Earth Surface Processes and Landforms*, *28*, 739–755. https://doi.org/10.1002/esp.495

Tonelli, M., Fagherazzi, S., & Petti, M. (2010). Modeling wave impact on salt marsh boundaries. *Journal of Geophysical Research, Oceans*, *115*. n/a-n/a. https://doi.org/10.1029/2009JC006026

Van den Boogaard, H. F. P., Uittenbogaard, R. E, Mynett, A. (2003). Construction of time series with prescribed statistical properties for applications in hydraulic engineering. Proceedings XXX IAHR Congress, Theme D: Hydroinformatics and advanced data technology in engineering practice", Korfiatis G. & Christodoulou, G. (Eds.), ISBN 960–243–598-1, pp. 107–114, August 2003.

Van den Hurk, B., Siegmund, P., Klein Tank, A., Attema, J. (2014). KNMI'14: Climate change scenarios for the 21st century—A Netherlands perspective.

van der Deijl, E. C., van der Perk, M., & Middelkoop, H. (2017). Establishing a sediment budget in the newly created 'Kleine Noordwaard' wetland area in the Rhine-Meuse delta. *Earth Surface Dynamics Discussion*, *2017*, 1–23. https://doi.org/10.5194/esurf-2017-22

Van der Werf, K. M. (2016). Implementing vegetation development into a quantitative hydromorphological model - A case study of inundated polder "Kleine Noordwaard" in the Biesbosch (the Netherlands).

Van Rijn, L. (1984). Sediment transport, Part II: Suspended load transport. *Journal of Hydraulic Engineering*, *110*, 1613–1641. https://doi.org/10.1061/(ASCE)0733-9429(1984)110:11(1613)

Van Velzen, E. H., Jesse, P., Cornelissen, P., Coops, H. (2003). Stromingsweerstand vegetatie in uiterwaarden. Deel 2 achtergronddocument versie 1–2003. RIZA rapport 2003.029.

Vandenbruwaene, W., Maris, T., Cox, T. J. S., Cahoon, D. R., Meire, P., & Temmerman, S. (2011). Sedimentation and response to sea-level rise of a restored marsh with reduced tidal exchange: Comparison with a natural tidal marsh. *Geomorphology*, *130*, 115–126. https://doi.org/10.1016/j.geomorph.2011.03.004

Verschelling, E., Van der Deijl, E. C., Van der Perk, M., Sloff, K., & Middelkoop, H. (2017). Effects of discharge, wind and tide on sedimentation in a recently restored tidal freshwater wetland. *Hydrological Processes*, *31*, 2827–2841.

Vollmer, S., & Goelz, E. (2006). Sediment monitoring and sediment management in the Rhine River. In *Sediment dynamics and the hydromorphology of fluvial systems*. Dundee, UK: IAHS.

How to cite this article: Verschelling E, van der Perk M, Middelkoop H. The impact of climate change on the morphology of a tidal freshwater wetland affected by tides, discharge, and wind. *River Res Applic*. 2018;34:516–525. https://doi.org/10.1002/rra.3282